to occultation effects. Thus, the inner disk in these dwarf novae must be radically different in structure from that predicted by theory (see ref. 10). Such a change in slope could be due to a breakdown of the thin disk approximation. If the disk became thick it would radiate as a rapidly rotating star[10]. This would satisfy the observed far-UV energy distribution (Fig. 2) and could explain the absence of evidence for a boundary layer through occultation effects and/or reprocessing of radiation.

With the outburst flux distribution for SS Cyg (Fig. 2) a bolometric luminosity can be computed. The shape of the far-UV distribution suggests that only a small amount of energy ($\lesssim 15\%$) is intrinsically emitted shortward of 912 Å. We find that the luminosity for SS Cyg in outburst is $1.3 \pm 0.3 \times 10^{34}$ erg s^{-1} ($\sim 3.3\ L_{\odot}$), assuming a distance of 50 pc (ref. 11). Similar arguments can be made for U Gem. However, the absence of adequate ground-based data makes the resultant luminosity very uncertain. Assuming a 3,000–10,000 Å distribution similar to that of SS Cyg, a luminosity of $1.5 \pm 0.5 \times 10^{34}$ erg s^{-1} is derived for a distance of 75 pc (ref. 12).

As discussed earlier, the only difference between the SS Cyg and U Gem far-UV flux distributions is the presence of Lyman series hydrogen absorption in SS Cyg. [Note neither SS Cyg nor U Gem show any suggestion of He II (specifically 1,085 Å) absorption.] The identification of this line as Lyβ and not O VI is based on the results of a division of the SS Cyg distribution by that of U Gem. This division revealed additional weak absorptions at Lyγ and Lyδ. The data from the earlier outburst observed in SS Cyg with Voyager also show Lyβ absorption. Although in this outburst the line is quite variable in strength. We postulate that most of the observed hydrogen absorption in SS Cyg originates in a wind. Such winds have been observed in other dwarf novae of low inclination[13]. The absence of wind lines in U Gem is also consistent with this model. Interstellar Lyβ is also a likely contributor to the absorption in SS Cyg. However, the observed variability of the feature suggests that it cannot be the principle source of the line.

The principal results from the Voyager UVS investigation of SS Cyg and U Gem in outburst can be summarized as follows. The far-UV light curve confirms the earlier observation of a delay in the rise of flux at shorter wavelengths relative to that occurring at longer wavelengths in the early stages of an outburst. The flux distribution in the far-UV is significantly flatter ($F_{\lambda} \propto \lambda^{-0.5 \pm 0.5}$) than that in the near-UV (IUE) region. No extreme-UV emission was detected in either SS Cyg or U Gem and the shape of their far-UV flux distributions suggest that little intrinsic extreme-UV flux is emitted. A bolometric luminosity of $1.3 \pm 0.3 \times 10^{34}$ erg s^{-1} is derived for SS Cyg in outburst ($d = 50$ pc). A similar luminosity, $1.5 \pm 0.5 \times 10^{34}$ ergs s^{-1}, is deduced for U Gem ($d = 75$ pc). No evidence is found for any significant area of the inner disk/boundary layer region with a temperature in excess of ~50,000 K. The far-UV flux distribution can be best represented by a high gravity ($\log g \sim 6$–8) intermediate temperature ($T_{\rm eff} \sim 50{,}000$ K) stellar atmosphere. These results argue for a significantly different inner disk/boundary layer structure than current theory predicts. Further observations of cataclysmic variables, simultaneous with observations for IUE and ground-based telescopes, are planned.

Received 23 January; accepted 14 March 1984.

1. Broadfoot, A. L. *et al. Space Sci. Rev.* **21**, 183–205 (1977).
2. Holberg, J. B., Forrester, W. T., Shemansky, D. E. & Barry, D. C. *Astrophys. J.* **257**, 656–671 (1982).
3. Eason, E. E. & Worden, S. P. *Publ. astr. Soc. Pacif.*, **95**, 58–60 (1983).
4. Hassall, B. J. M. *et al. Mon. Not. R. astr. Soc.* **203**, 865–885 (1983).
5. Oke, J. B. & Wade, R. A. *Astr. J.* **87**, 670–679 (1982).
6. Panek, R. J. & Holm, A. V. *Astrophys. J.* **277**, 700–709 (1984).
7. Córdova, F. A. & Mason, K. O. in *Accretion Driven Stellar X-ray Sources* (eds Lewin, W. H. G. & ven den Heuval, E. P. J.) (Cambridge University Press, 1982).
8. Córdova, F. A., Chester, T. J., Mason, K. O., Kahn, S. M. & Garmire, G. P. *Astrophys. J.* (in the press).
9. Ritter, H. *Catalogue of Cataclysmic Binaries, Low-Mass X-Ray Binaries and Related Objects* (Max-Planck-Institut für Physik und Astrophysik, Garching, 1983).
10. Pringle, J. E. *A. Rev. Astr. Astrophys.* **19**, 137–162 (1981).
11. Kamper, K. W. in *White Dwarfs and Variable Degenerate Stars* (eds Van Horn, H. M. & Weidemann, V.) 494 (University of Rochester Press, 1979).
12. Wade, R. A. *Astr. J.* **84**, 562–566 (1979).
13. Córdova, F. A. & Mason, K. O. *Astrophys. J.* **260**, 716–721 (1982).

Upper limit on solar interior rotation

Martin Woodard

Center for Astrophysics and Space Sciences, University of California, San Diego, La Jolla, California 92093, USA

The power spectrum of solar total irradiance (flux) variations from the Active Cavity Radiometer Irradiance Monitor (ACRIM) on the Solar Maximum Mission (SMM) spacecraft shows individual 5-min *p*-mode oscillations[1,2] of spherical harmonic degree $l = 0$–2 and radial order $n = 16$–26. An *m*-state splitting analysis based on the widths of the (n, l) multiplets in the spectrum of ACRIM data yields a mean (sidereal) interior rotation rate between 0 and 2.2 times the observed 0.456-μHz equatorial surface rate, consistent with the rapid rotation rate originally claimed by Claverie *et al.*[3] based on a (controversial) splitting interpretation of the these 5-min modes seen in line-of-sight velocity. Rotationally split *p*- and *g*- and *f*-modes have been identified in the temporal power spectrum of the limb-darkening data of Bos and Hill[4], and from these splittings two internal rotation curves[5,6] have been deduced which imply a solar gravitational quadrupole moment J_2 large enough to spoil the precise agreement between general relativity and observations of planetary motion. The splitting of the low-l 5-min *p*-modes implied by these curves is inconsistent with the upper limit derived here, and the reported conflict with einsteinian theory, is therefore, premature.

In this analysis I assume that the fluid angular velocity within the Sun has a radial dependence of the form $\mathbf{\Omega} = \Omega(r)\hat{z}$. The axis $\hat{z}$ is known from surface motion. For a rotation law of this form, the frequency of a free-oscillation mode depends on the quantum numbers (nlm) of the mode as[7]:

$$\nu_{nlm} = \nu_{nl} + m\Delta_{nl} \tag{1}$$

where Δ_{nl}, defined in an inertial frame, is an integral over radius of $\Omega(r)$ times a weighting function. Explicit expressions for the weighting functions, or splitting kernels, are given in ref. 7. (Other sources of splitting, such as a magnetic field, will be ignored in this analysis.) For rotation curves which are suitably smooth functions of r, the low-l 5-min p-mode splitting is adequately approximated by the expression[8]

$$\Delta = \int_0^R \frac{\Omega(r)}{2\pi} \frac{\mathrm{d}r}{c(r)} \Big/ \int_0^R \frac{\mathrm{d}r}{c(r)} \tag{2}$$

in which $c(r)$ is the sound speed at radius r. I further assume that the modes are excited independently and isotropically, and that the mean energy per (nlm) mode depends only on frequency, in accordance with the overall distribution of power in peaks of different l as observed in the power spectrum of both the Nice data[8,9] and the ACRIM data.

The present conclusions come from measurements of the width of several $l = 0$ and 1 peaks near the maximum of the 5-min mode excitation envelope (~3,100 μHz). The $l = 2$ peaks were not quantitatively analysed because of their small signal-to-noise ratio. Because the axis $\hat{z}$ is nearly perpendicular to our line-of-sight, only even $l + m$ components should be visible in whole-disk measurements. I therefore assume the underlying line profile (in excess of background) of each $l = 1$ peak to be a superposition of two identical lobes, representing the $m = \pm 1$ components. The observable separation of the lobes, S, is related to the sidereal splitting Δ in equation (1) by

$$S = 2(\Delta - \nu_{\rm e}) \tag{3}$$

where $\nu_{\rm e} \approx 0.03$ μHz is the orbital frequency of the Earth about the Sun. The separate lobes are assumed to have lorentzian line shapes. The $l = 0$ peaks are represented by a single such lobe. Defining the linewidth as the width of a symmetrically placed bin containing half the power in the line[2], the width of the assumed doublet profile, W_1, the width of the individual lobes,

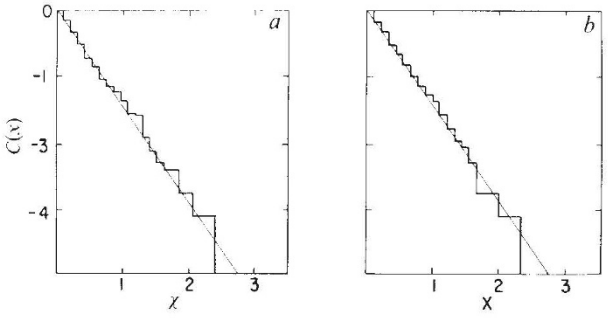

Fig. 1 *a*, The logarithm $C(x)$ of the fraction of frequency points for which the spectral power estimate p'_ν exceeds the true power by the factor x (arbitrary units), plotted for frequencies taken from 1.86-μHz bandwidth intervals centred on 5-min p-mode resonances in the periodogram of ACRIM data. (The true spectral power p_ν was determined from the mode parameter estimation scheme of ref. 2.) Eight intervals were selected, corresponding to the peaks $l=0$, $n=20$–23 and $l=1$, $n=19$–22. The frequency sampling of the periodogram is 29.1038 nHz so that 64 frequencies per mode were used. *b*, $C(x)$ plotted from 512 frequencies belonging to a background interval in the 5-min range. The linearity of these plots corresponds to a χ^2 distribution with 2 degrees of freedom, the distribution assumed in the error analysis. (This method of display was suggested by P. Delache.)

W_0, and the separation, S, obey a pythagorean relationship:

$$W_1^2 = W_0^2 + S^2 \quad (4)$$

The differences between the shapes of 5-min peaks in the ACRIM data and the idealized line profiles discussed above are assumed to be mainly statistical: thus linewidth measurements are subject to random error. Accordingly, I assume that the spectral power estimates p'_ν at frequencies separated by more 0.04 μHz (the resolution of 290 days of data) are uncorrelated, and that p'_ν at each frequency ν comes from a χ^2 distribution with 2 degrees of freedom, a distribution typical of a periodogram of filtered noise. The mean of the χ^2 distribution, p_ν (the true spectral power that p'_ν estimates), presumed to be a superposition of idealized 5-min mode profiles and a nearly flat background 'continuum', was estimated from the parameters of the individual 5-min modes[2] and the observed continuum.

Two tests demonstrate the credibility of these statistics. To check that the periodogram conforms to the stated distribution I have plotted $C(x)$ against x in Fig. 1, where $\exp\{C(x)\}$ is the fraction of periodogram points for which p'_ν/p_ν exceeds x. The straight line plots confirm the expected $C(x) \propto -x$ dependence, both for frequency intervals containing 5-min modes and for background intervals. To verify the statistical independence of the spectral estimate at frequencies differing by more than 0.04 μHz, I smoothed the periodogram and measured the decrease in the scatter of the points. The ratio of the variance in the smoothed periodogram to that in the original should equal 0.04 μHz divided by the effective resolution of the smoothed periodogram. This dependence was confirmed for frequency ranges of interest.

The operational definitions of power and linewidth[2] systematically underestimate the true power and width because the power in the modes is integrated only over a 5-μHz interval. A Monte Carlo simulation was performed to calibrate empirically the relation between the true power and width of the $l=0$ modes and the expected value of the operationally defined power and width, and to determine the random error of the measurement. In this, and in subsequent simulations, a statistical ensemble of artificial periodograms containing modes and background were generated with the statistical properties assumed for the real data. Ignoring the possible variation of linewidth with frequency, the true width inferred for the four strongest $l=0$ lines ($n=$ 20–23) is $\Delta\nu = 1.6 \pm 0.3$ μHz.

A second Monte Carlo calculation calibrated the relation between the width W_1 and power of the $l=1$ doublets and the operationally-defined linewidth and power, assuming that the

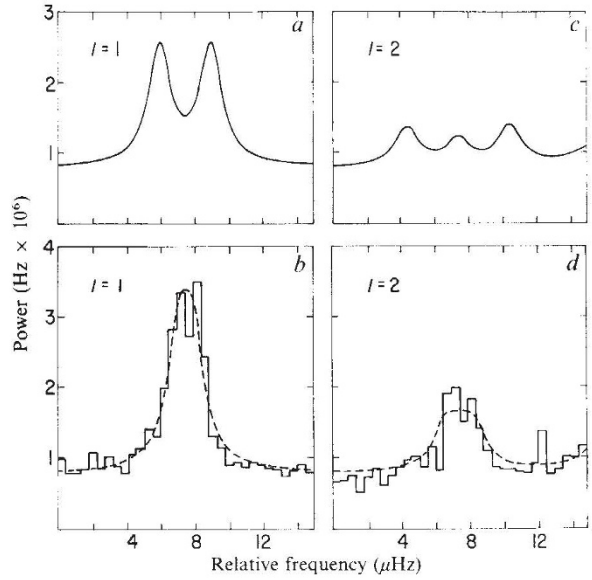

Fig. 2 *a*, Theoretical $l=1$ profile with a lobe separation of 3.0 μHz, that is a splitting $\Delta = 1.56$ μHz as defined in the text, slightly less than the separation implied by the rotation curves of refs 5 and 6. The total power in the doublet equals the mean power of the $l=1$ modes studied in this analysis and the width of the lobes equals the estimated 1.6-μHz width of the $l=0$ modes in the same frequency range. The continuum power level is that of the ACRIM data. The theoretical line shape corresponding to the larger splitting stands in marked contrast to the appearance of the actual modes. *b*, Superposition of three $l=1$ peaks ($n=20$–23) in the ACRIM periodogram, based on the measured frequency centroids, plotted at a resolution of 0.4657 μHz. The smooth curve is a doublet with a (synodic) lobe separation $S=0.86$ μHz, the separation expected from solid-body rotation with a ~25-day sidereal period and represents the theoretical appearance of a smoothed periodogram based on an unlimited amount of data. *c*, Idealized $l=2$ profile resulting from the $\Delta = 1.56$-μHz splitting is also at variance with the data and further substantiates our conclusions. The relative power 3:2:3 in the $m=-2$, 0, and +2 lobes shown and the absence of the $m=\pm1$ lobes in full-solar-disk measurements is dictated by isotropy and by the assumption of a solar rotation axis perpendicular to our line of sight. *d*, The superposition of the four $l=2$ modes ($n=19$–22) is also consistent solid-body rotation (the smooth curve again indicates the theoretical profile which best fits the data).

doublet components have the same width as the $l=0$ modes in the same frequency range (that is, $W_0 = \Delta\nu$). This gives a mean width for the three $l=1$ modes ($n=20$–22) of $W_1 = 1.9 \pm 0.2$ μHz. A composite of the three observed $l=1$ modes appears in Fig. 2. The value of Δ inferred from W_0 and W_1 through equations (3) and (4) is 0.5 (+0.2, −0.5) μHz, consistent with the 0.456-μHz splitting expected from solid-body rotation with a ~25-day sidereal period, but also consistent with any rotational rate between 0 and 1.4 times the surface rate (1σ error limits). Note that only the magnitude of S (in equation (3)) can be determined from the (full-disk) ACRIM data. An unambiguous value for Δ was obtained by assuming that S is positive, in accordance with a net internal rotation having the same sense as the surface rotation.

Relaxing the assumption $W_0 = \Delta\nu$, made above, leads to a more rigorous upper bound on splitting. The probability of obtaining an $l=1$ linewidth smaller than the observed one, for various hypothetical values of Δ, was computed from a Monte Carlo program. In this final program, the influence of oscillations aliased into the 2,900–3,300-μHz range by the ACRIM shutter operation[2] was also simulated. Based on the published analysis of the Nice group[10], whose velocity oscillation spectrum extends well beyond the 3,814.7-μHz ACRIM Nyquist limit, the spectral power per multiplet of given l is at least three times greater at the frequencies of interest than at the frequencies of multiplets that would produce aliases. The m-state width of the potentially aliased multiplets is assumed to be 5 μHz. For each point on a

grid of mode parameters (Δ, W_0, and parameters defining the power and frequency of the aliases) a number of trial measurements were performed. A trial consists of generating three independent periodograms based on the same profile, measuring the doublet width in each, and averaging the three measurements. For $\Delta = 1.0$ and 2.0 μHz, 256 and 1,024 trials were made, respectively, for each value of the other parameters. (The ranges of the other parameters reflect their uncertainty, in particular W_0 was assumed to lie in the range 0.6–1.8 μHz.) At the lower splitting only one trial (at most) per grid point resulted in a mean width smaller than the observed one, and at the larger splitting there were no such occurrences. I thus infer a strong ($\approx 2.5\sigma$) upper limit $\Delta_{max} = 1.0$ μHz on the rotational splitting.

These results demand comparison with internal rotation curves obtained from different analyses of rotationally split modes in the solar limb-darkening data[4]. Hill *et al.*[5] have derived a rotation curve from these data which implies a solar mass quadrupole moment $J_2 = (5.5 \pm 1.3) \times 10^{-6}$, in conflict with the einsteinian general relativistic interpretation of Mercury's perihelion motion at the 2σ level. From a preliminary analysis of the same data, Gough[7] obtained $J_2 = 3.6 \times 10^{-6}$, not large enough to conflict with general relativity. Both analyses used seven multiplets for the curve fitting, a common set with the exception of two p-modes. A more recent analysis by Campbell *et al.*[6] essentially confirms the Hill *et al.* rotation curve, giving $J_2 = 5.0 \times 10^{-6}$, again in conflict with relativistic predictions.

To test the conclusions derived from the limb-darkening data I have calculated, using equation (2), the splitting of the low-l 5-min modes implied by the curves used to derive the quoted J_2 values. The function $c(r)$ was taken from a recent standard solar model calculation[11]. The rotation curves in refs 7, 5, and 6 imply $\Delta = 1.46$, 1.70, and 1.69 μHz, respectively, in conflict with the upper limit $\Delta_{max} = 1.0$ μHz derived here. Thus the basis established in refs 5 and 6 for conflict between general relativity and solar oscillation data is removed by the SMM data.

I thank Richard C. Willson for making the ACRIM data available, Roger Ulrich for supplying the results of solar model calculations, and A. N. McClymont for suggesting improvements in the manuscript. This research was suggested by Hugh Hudson and supported by NASA on grant NSG 7161.

Received 23 January; accepted 2 April 1984.

1. Woodard, M. & Hudson, H. S. *Sol. Phys.* **82**, 67–73 (1983).
2. Woodard, M. & Hudson, H. S. *Nature* **305**, 589–593 (1983).
3. Claverie, A., Isaak, G. R., McLeod, C. P., van der Raay, H. B. & Roca Cortes, T. *Nature* **293**, 443–445 (1981).
4. Bos, R. J. & Hill, H. A. *Sol. Phys.* **82**, 89–102 (1983).
5. Hill, H. A., Bos, R. J. & Goode, P. R. *Phys. Rev. Lett.* **49**, 1794–1797 (1982).
6. Campbell, L., McDow, J. C., Moffat, J. W. & Vincent, D. *Nature* **305**, 508–510 (1983).
7. Gough, D. O. *Nature* **298**, 334–339 (1982).
8. Christensen-Dalsgaard, J. & Gough, D. O. *Mon. Not. R. astr. Soc.* **198**, 141–171 (1982).
9. Grec, G., Fossat, E. & Pomerantz, M. *Nature* **288**, 541–547 (1980).
10. Grec, G., Fossat, E. & Pomerantz, M. *Sol. Phys.* **82**, 55–66 (1983).
11. Ulrich, R. K. & Rhodes, E. J. Jr *Astrophys. J.* **265**, 551–563 (1983).

A new imaging proportional counter using a Penning gas improves energy resolution

H. E. Schwarz & I. M. Mason

Mullard Space Science Laboratory, University College London, Holmbury St Mary, Dorking, Surrey RH5 6NT, UK

In recent years Siegmund *et al.*[1,2] have attempted to combine in one detector the position resolution of the multi-wire proportional counter (MWPC)[3–5] or the parallel-plate imaging proportional counter (PPIPC)[6,7] with the energy resolution of the gas-scintillation proportional counter (GSPC)[8–11], using light from avalanches in a PPIPC. By counting the light flashes from individual primary electrons, Fano factor limited energy resolution was obtained but only for energies below 2 keV. The position resolution was $\approx$350 μm over an active diameter of 25 mm. Sipilä and co-workers[12,13] used Penning gas[14,15] mixtures to improve the energy resolution to 11% at 6 keV. However, this was achieved at gas gains of <50, and in a single wire proportional counter (PC) without imaging capability. We have achieved similar resolution with gains up to 550 by using a Penning gas in a uniform field. Although satisfactory for energy measurement down to 0.1 keV this gain is not high enough for good position resolution in a PPIPC. We therefore use another stage of uniform field avalanching to boost the overall gain to values $>10^5$. The concept of two-stage avalanching was first reported by Charpak *et al.*[16] and used by Breskin *et al.*[17]. We have built and tested a laboratory version of such a detector (Fig. 1), which we call the Penning gas imager (PGI). A Penning gas and a two-stage parallel grid avalanche geometry are combined with a wedge and strip anode (WSA) position read-out system[18]. Preliminary experimental energy resolution is 12% FWHM at 6 keV (24% FWHM at 1.5 keV) and the position resolution is 100 μm FWHM at 1.5 keV. This compares with $\approx$10% and $\approx$1 mm for the GSPC and $\approx$18% and a few hundred micrometres for the MWPC. The particle background can be reduced by an estimated 99% using an anticoincidence technique.

The energy resolution of a PC is limited by both Fano and avalanche statistics. The FWHM resolution is given by

$$R_E(\%) = 236[w(F + f + g)/E]^{0.5}$$

where w is the mean energy to produce one ion pair, F the Fano factor, f the avalanche factor, g a broadening factor depending on the small scale grid or wire geometry, and E is the X-ray energy.

The value of F for argon (and conventional PC gas mixtures such as Ar/CH_4) is 0.17 and f is typically 0.65 (ref. 19). With $w = 26.2$ eV in argon this gives $R_E = 35E^{-1/2}$ where E is in keV. This assumes $g = 0$. In practice this resolution is not achieved due to irregularities in the anode wires[20] or the grids[7]; 18% at 6 keV is a typical value and this implies a g factor equivalent to 10% extra broadening.

In the GSPC the f and g factors are eliminated by not using avalanches. In principle, $R_E = 16E^{-1/2}$ can be achieved but a typical observed value at 6 keV is 10% compared with a theoretically possible 6%. This corresponds to an additional broadening of about 8% due to gas impurities and geometry dependent light losses in the counter.

The energy resolution of the PGI is potentially as good as that of the GSPC. By using argon with the Penning admixture C_2H_2 which has an ionization potential lower than the energy of the photons emitted by the excited Ar atoms, the admixture can be photo-ionized. Also metastable argon atoms can collisionally ionize the ethyne molecules. This process, known as the Penning effect, produces a dramatic increase in α, the first Townsend coefficient[15]. As an example, the changes in the relative efficiencies of the various processes such as excitation and ionization in a Ne/Ar mixture are shown in Fig. 2. In the initial ionization, more of the available energy of the primary photo-electron and Auger electron is used for ionization (the value of w is reduced from 26.2 to 20.3 eV)[19] and in addition the fluctuations in the energy losses are smaller. The Fano factor is thus reduced[19].

In the avalanche, using the model of Alkhazov[19] and the data on α of Kruithof and Penning, Sipilä[13] shows that for an optimum value of the field strength, f approaches zero in a (Penning) mixture of Ne and Ar. As the process for Ar/C_2H_2 is similar such a result can also be expected for this mixture. A theoretical energy resolution of $10E^{-1/2}$ is then available. Sipilä's results were obtained at low gas gains (<50) but the resolution in conventional PCs rapidly degrades with increasing gain. This is due to the strongly varying field near the anode wire which makes it impossible to use the optimum field[15,19] needed for low values of f. Sipilä was aware of this limitation and suggested the use of a uniform field avalanche[13]. In the PGI the parallel geometry provides a uniform field and much higher gains can